

# miR-340-5p Suppresses Aggressiveness in Glioblastoma Multiforme by Targeting Bcl-w and Sox2

Sanghwa Kim,<sup>1,3</sup> Jae Yeon Choi,<sup>1,3</sup> Hyun Jeong Seok,<sup>1</sup> Myung-Jin Park,<sup>1</sup> Hee Yong Chung,<sup>2</sup> and In Hwa Bae<sup>1</sup>

<sup>1</sup>Division of Radiation Biomedical Research, Korea Institute of Radiological & Medical Science, Seoul, Republic of Korea; <sup>2</sup>Department of Microbiology, College of Medicine, Hanyang University, Seoul, Republic of Korea

**Glioblastoma multiforme (GBM), a particularly aggressive type of malignant brain tumor, has a high mortality rate. Bcl-w, an oncogene, is reported to enhance cell survival, proliferation, epithelial-mesenchymal transition (EMT), migratory and invasive abilities, and stemness maintenance in a variety of cancer cell types, including GBM. In this study, we confirmed that Bcl-w-induced conditional medium (CM) enhances tumorigenic phenotypes of migration, invasiveness, and stemness maintenance. Notably, platelet-derived growth factor-A (PDGF-A) expression, among other factors of the tumor environment, was increased by CM of Bcl-w-overexpressing cells, prompting investigation of the potential correlation between Bcl-w and PDGF-A and their effects on GBM malignancy. Bcl-w and PDGF-A levels were positively regulated and increased tumorigenicity by Sox2 activation in GBM cells. miR-340-5p was further identified as a direct inhibitor of Bcl-w and Sox2. Overexpression of miR-340-5p reduced mesenchymal traits, cell migration, invasion, and stemness in GBM through attenuating Bcl-w and Sox2 expression. Our novel findings highlight the potential utility of miR-340-5p as a therapeutic agent for glioblastoma multiforme through inhibitory effects on Bcl-w-induced PDGF-A and Sox2 activation.**

## INTRODUCTION

Glioblastoma multiforme (GBM) is a lethal type of astrocytic brain tumor associated with a high mortality rate.<sup>1-4</sup> Although the molecular mechanisms underlying GBM progression and treatment strategies have been extensively investigated, effective treatment of brain tumors remains a considerable clinical challenge.<sup>2,5,6</sup> Progression of brain tumors is affected by the tumor microenvironment, which is closely associated with the relationships between cancer cells and multiple factors, including cytokines, chemokines, and growth factors, secreted from stromal cells.<sup>7</sup> Glioma cells affected by tumor microenvironment-related factors are reported to exhibit malignant phenotypes, including infiltration, and accelerate cancer progression.<sup>7,8</sup>

Bcl-w is highly expressed in various cancers, including gastric cancer,<sup>9</sup> colorectal adenocarcinoma,<sup>10</sup> and GBM.<sup>11,12</sup> Our previous studies have indicated that Bcl-w acts as an oncogene contributing to tumorigenicity and metastasis as well as cell survival.<sup>11,12</sup> However, the

mechanisms by which Bcl-w regulates malignancy in GBM remain to be established.

microRNAs are small non-coding RNAs that regulate gene expression via translational inhibition.<sup>13,14</sup> Moreover, miRNAs are involved in pathways regulating multiple physiological processes, such as cell proliferation, apoptosis, invasion, metastasis, angiogenesis, and the resistance to radio- and chemotherapy,<sup>3</sup> and can act as either oncogenes or tumor suppressors.<sup>1,15</sup> miRNAs may serve as biological tools or provide important information for cancer diagnosis based on their ability to regulate gene expression.<sup>15</sup> Therefore, the detailed mechanism analysis of miRNAs in GBM may be useful in developing more effective strategies for cancer diagnosis and potential biomarker discovery.

In the current study, we analyzed Bcl-w-induced microenvironmental factors and their interrelationships, with a view to clarifying the mechanistic pathways underlying malignant transformation by Bcl-w. Based on the collective findings, we have put forward a potential strategy for the treatment of GBM using miR-340-5p that blocks the mechanism of action of Bcl-w.

## RESULTS

### Conditioned Media (CM) from Bcl-w-Overexpressing Cells Promote Tumorigenicity in GBM

We have previously established that Bcl-w contributes to the mesenchymal properties of GBM.<sup>12</sup> To determine whether Bcl-w-induced alterations in the tumor microenvironment promote malignancy, U87 and U251 cells were treated with CM collected from Bcl-w-overexpressing GBM. Expression of the epithelial-mesenchymal transition (EMT)-related genes, such as Vimentin, Twist, and Snail, was increased in U87 and U251 treated with Bcl-w-overexpressing CM

Received 18 December 2018; accepted 24 May 2019;  
<https://doi.org/10.1016/j.omtn.2019.05.022>.

<sup>3</sup>These authors contributed equally to this work.

**Correspondence:** In Hwa Bae, PhD, Division of Radiation Biomedical Research, Korea Institute of Radiological & Medical Sciences, 75 Nowon-ro, Nowon-gu, Seoul 01812, Republic of Korea.

**E-mail:** [ihbae@kirams.re.kr](mailto:ihbae@kirams.re.kr)



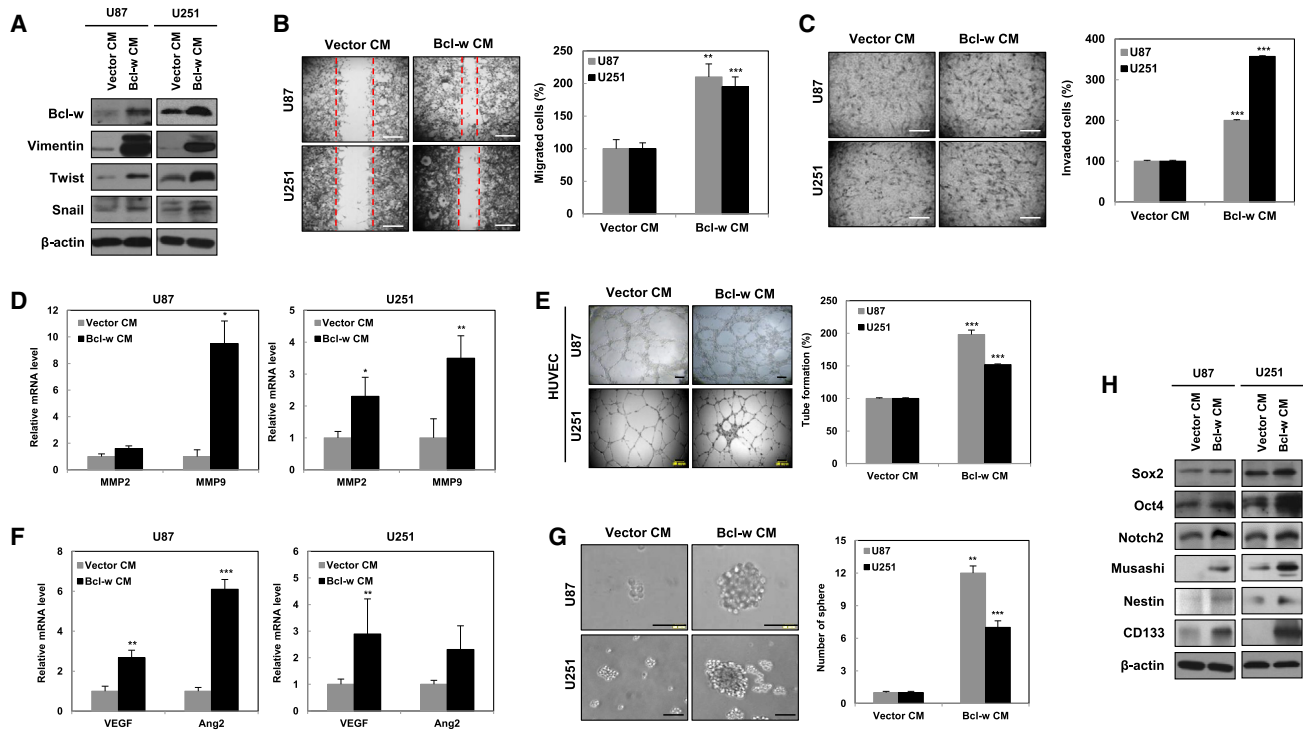


**Figure 1. Conditioned Media from Bcl-w-Transfected Cells Promote Tumorigenicity in Glioblastoma Multiforme, U87, and U251 Cells**

After U87 and U251 cells were transfected with control vector or Bcl-w, each conditioned media (CM) was collected. And then U87 and U251 cells were treated with vector CM or Bcl-w CM for 24 h. (A) Mesenchymal marker proteins including Vimentin, Twist, and Snail were detected in U87 and U251 cells treated with vector CM or Bcl-w CM by western blot assay.  $\beta$ -actin was used as a loading control in all data of western blot assay. (B–D) The migratory (B) and invasive abilities (C) and their related enzymes, MMP-2/9 (D), of vector or Bcl-w CM-treated U87 and U251 cells were examined by wound healing (scale bars, 100  $\mu$ m), matrigel invasion assay (scale bars, 100  $\mu$ m), and qRT-PCR. GAPDH mRNA was used for normalization. (E) After HUVECs (human umbilical vein endothelial cells) were resuspended in CM from vector or Bcl-w-transfected U87 and U251 cells and seeded on matrigel-coated plates, tube-formation assay was conducted for 6 h (scale bars, 100  $\mu$ m). (F) After U87 and U251 cells were treated with each CM from vector or Bcl-w-transfected cells, levels of angiogenesis-related mRNA such as VEGF (vascular endothelial growth factor) and Ang2 (angiopoietin-2) expression were detected by qRT-PCR. (G and H) U87 and U251 cells treated with vector or Bcl-w CM were determined sphere-forming ability (G) and stemness-related protein expressions, Sox2, Oct4, Notch2, Musashi, Nestin, and CD133 (H) by sphere-formation assay (G; scale bars, 100  $\mu$ m) and western blot assay. The data are presented as the mean  $\pm$  SD. \* $p < 0.05$ , \*\* $p < 0.01$ , and \*\*\* $p < 0.001$ . Student's *t* test.

(Figure 1A). Migratory and invasive activities of these cells were additionally enhanced, compared with CM of vector-transfected cells (Figures 1B and 1C). Moreover, mRNA levels of matrix metalloproteinases (MMPs), such as MMP-2 and MMP-9 involved in invasive ability, were elevated in cells treated with CM of Bcl-w-overexpressing cells (Figure 1D). To determine the effects on endothelial cells due to Bcl-w-induced changes in the microenvironment, a tube formation assay *in vitro* was performed using human umbilical vein endothelial cells (HUVECs), which are a well-known model for the reorganization stage of angiogenesis.<sup>16</sup> HUVECs treated with CM of Bcl-w-overexpressing cells showed a dramatic increase in tube-formation ability relative to those treated with CM of vector-transfected cells (Figure 1E). mRNA levels of angiogenesis-related factors, including angiopoietin-2 (Ang2) and vascular endothelial growth factor (VEGF), were significantly increased in U87 and U251 cells treated with Bcl-w overexpressing CM, compared to the vector-transfected control group (Figure 1F). Next, Bcl-w-overexpressing CM additionally contributed to increased sphere-formation ability in the two

GBM cell lines (Figure 1G). Sphere-formation assay is known as a method to confirm the stemness maintenance, one of the cancer malignant features.<sup>17–19</sup> Sox2, Oct4, and Notch2,<sup>20,21</sup> together with Musashi-1, Nestin, and CD133, are known as cancer stem-like cell markers in GBM.<sup>22,23</sup> Expression levels of cancer stem-like cell-related proteins, such as Sox2, Oct4, Notch2, Musashi-1, Nestin, and CD133, were dramatically increased in U87 and U251 treated with Bcl-w-overexpressing CM (Figure 1H).

#### Positive Regulation between PDGF-A and Bcl-w Promotes Aggressiveness of GBM

Cancer cells alter the tumor microenvironment by secreting various growth factors and cytokines,<sup>24</sup> leading to acquisition of malignancy. To investigate the mechanisms underlying the aggressiveness of GBM, we analyzed various factors from CM that may have induced changes in the tumor microenvironment. Since growth factors regulate a variety of cellular processes, such as proliferation, differentiation, and progression,<sup>25–27</sup> the mRNA levels of MCP3 (monocyte-chemotactic

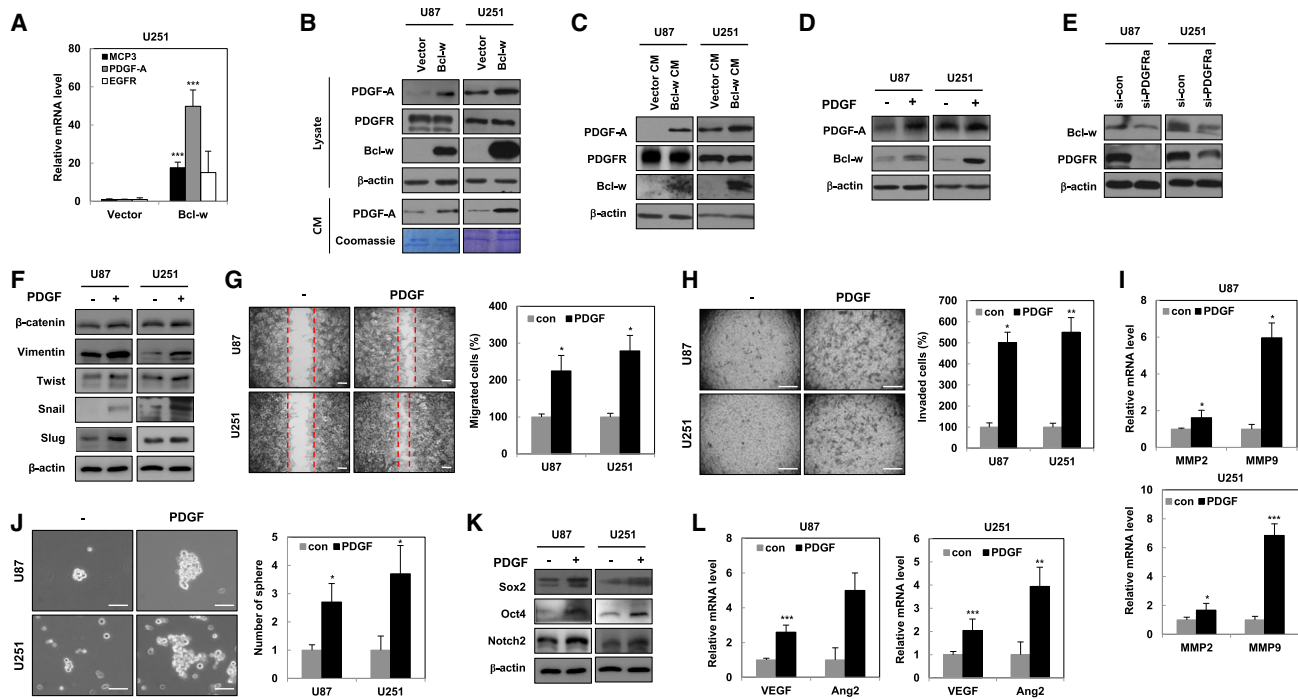


**Figure 2. The Positive Regulation of Bcl-w and PDGF-A Induces Aggressiveness in GBM**

(A) Levels of MCP3, PDGF-A, and EGFR mRNA were measured in control vector or Bcl-w-overexpressing U251 cells by qRT-PCR analysis. (B and C) PDGF-A protein expressions were detected in lysates or CM obtained from control vector and Bcl-w-overexpressing cells (B) and GBM cells treated with CM from Bcl-w-overexpressing cells (C) by western blot assay. Coomassie Blue staining or  $\beta$ -actin was used as loading control. (D and E) After U87 and U251 cells were incubated with or without PDGF (10 ng/mL) (D) or transfected by siRNA against PDGFR $\alpha$  (E), Bcl-w expression levels were detected by western blot assay. (F–L) Expressions of EMT-related proteins ( $\beta$ -catenin, Vimentin, Twist, Snail, and Slug) (F), mobility (G), invasiveness (H), mRNA levels of invasiveness-related enzymes (MMP-2 and MMP-9) (I), sphere-forming ability (J), expressions of cancer stem-like cell marker protein (Oct4, Sox2, and Notch2) (K), and expressions of angiogenesis-related factor mRNA (VEGF and Ang2) (L) were conducted by western blot assay, wound-healing assay (G; scale bars, 100  $\mu$ m), invasion assay (H; scale bars, 100  $\mu$ m), qRT-PCR analysis, and sphere-formation assay, respectively, in U87 and U251 cells following treatment of PDGF. The data are presented as the mean  $\pm$  SD. \* $p < 0.05$ , \*\* $p < 0.01$ , and \*\*\* $p < 0.001$ . Student's *t* test.

protein 3), PDGF-A (platelet-derived growth factor-A), and EGFR (epidermal growth factor receptor) were assessed (Figure 2A). We chose the most increased PDGF-A by Bcl-w. PDGF-A is known to be involved in cell growth, division, and angiogenesis.<sup>28</sup> Notably, we detected significant upregulation of PDGF-A relative to other factors in cell lysates and CM of Bcl-w-overexpressing U87 and U251 cells (Figure 2B). Moreover, PDGF-A levels were highly elevated in GBM cell lines treated with CM from Bcl-w-overexpressing cells (Figure 2C). We further examined the potential correlation between Bcl-w and PDGF-A with the aid of recombinant PDGF. Recombinant PDGF enhanced Bcl-w expression in both GBM cell lines, indicating a positive regulatory loop between the two molecules (Figure 2D). Next, we ascertained whether the positive feedback loop of PDGF-A and Bcl-w is regulated by the PDGF receptor (PDGFR) using PDGFR-specific small interfering RNA (siRNA) (Figure 2E). Bcl-w expression was clearly decreased upon transfection of cells with PDGFR-specific siRNA, suggesting that expression of Bcl-w is mediated through PDGF receptor signaling. Following treatment with recombinant PDGF, we investigated the phenotypes' change in U87 and U251 cells. Treatment with PDGF-induced expression of EMT-related proteins (Figure 2F) as well as migratory and invasive abilities (Figures 2G

and 2H) through enhancing MMP-2 and MMP-9 mRNA expression (Figure 2I), sphere-formation ability (Figure 2J), expression of cancer stem-like cell proteins, including Sox2, Oct4, and Notch2 (Figure 2K), and mRNA expression of the angiogenesis-related factors Ang2 and VEGF (Figure 2L) in U87 and U251 GBM cells. Our results clearly indicate that PDGF-A, which is secreted by Bcl-w-overexpressing cells, ultimately promotes aggressive GBM. Accordingly, we suggested that overexpression of Bcl-w in GBM induced changes in the tumor micro-environment and ultimately promoted tumor malignancy.

#### Sox2 Is Involved in Bcl-w-Induced Tumorigenicity of GBM Cells

Bcl-w dramatically increased expression of Sox2 not only in cells treated with CM of Bcl-w-overexpressing cells (Figure 1H) but also in Bcl-w-overexpressing cells (Figure S1). We described the signaling pathway for relationship between Bcl-w and Sox2 expression using siRNAs targeting Sox2 and Bcl-w. Sox2 knockdown using specific siRNAs was performed to confirm whether Bcl-w-induced Sox2 is involved in the aggressive phenotypes of the GBM cell lines U87 and U251. Levels of mesenchymal-related Vimentin, Snail, and Twist proteins (Figure 3A) as well as migratory (Figure 3B) and invasive activities (Figure 3C) of Bcl-w-overexpressing GBM cells were reduced

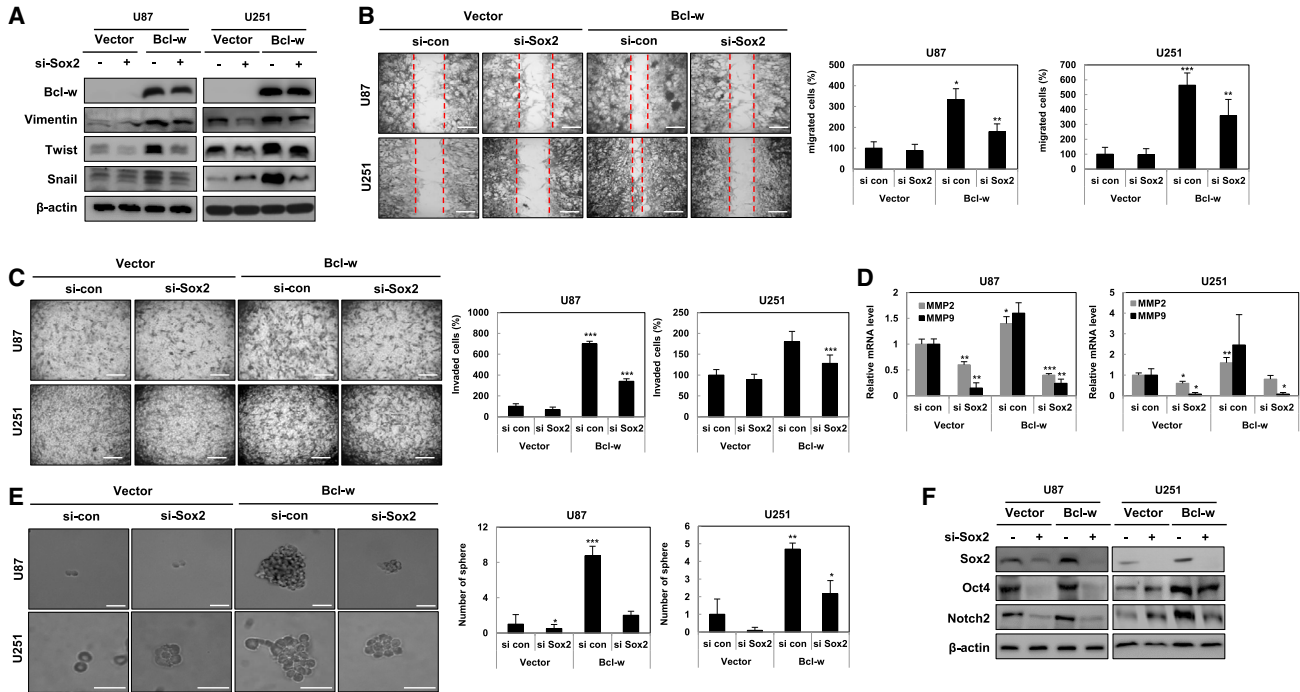


**Figure 3. Bcl-w Promotes Migration, Invasiveness, and Stemness by Regulating Sox2 Expression in GBM**

(A–F) After negative control or Bcl-w-overexpressing GBM cells were transfected with si-control or Sox2-specific siRNA for 48 h, mesenchymal-related protein expressions such as Vimentin, Twist, and Snail (A), migratory (B) and invasive activities (scale bars, 100  $\mu$ m) (C), mRNA levels of MMP-2 and MMP-9 as invasion-related factors (D), sphere-formation ability (E), and expressions of cancer stem-like cell marker proteins including Sox2, Oct4, and Notch2 (F) were determined by western blot assay, wound-healing assay (B; scale bars, 100  $\mu$ m), matrigel invasion assay (C; scale bars, 100  $\mu$ m), qRT-PCR analysis, and sphere-formation assay (E; scale bars, 100  $\mu$ m), respectively. The data are presented as the mean  $\pm$  SD. \* $p$  < 0.05, \*\* $p$  < 0.01, and \*\*\* $p$  < 0.001. Student's t test.

upon siRNA-mediated depletion of Sox2. In particular, Bcl-w-induced invasiveness was suppressed through downregulation of MMP-2 and MMP-9 mRNA expression (Figure 3D). Sox2 knock-down further attenuated Bcl-w-induced sphere-formation ability and expression of cancer stem-like cell-related marker proteins (Figures 3E and 3F). Meanwhile, overexpression of Sox2 did not change Bcl-w protein expression in U87 and U251 (Figure S2). Our collective results clearly support that Sox2 was involved in the Bcl-w-induced tumor malignant actions in GBM cells.

#### miR-340-5p Directly Downregulates Bcl-w and Sox2

##### Expressions

The above results clearly indicate that Bcl-w and Sox2 contribute to tumor progression of GBM. To investigate the potential miRNA profiles that regulate expression of these two proteins, we employed two miRNA target prediction programs, TargetScan (<http://www.targetscan.org>) and miRDB (<http://www.mirdb.org>). Consequently, miR-340-5p was found as a microRNA (miRNA) inducing significant suppression of Bcl-w and Sox2 expression (Figure 4A). Overexpression of a miR-340-5p mimic suppressed both Bcl-w and Sox2 protein and mRNA expression in U87 and U251 cells (Figures 4B–4D). Conversely, overexpression of miR-340-5p inhibitor (anti-miR-340-5p) increased both protein and mRNA expression of Bcl-w and Sox2 (Figures S3A–S3C). In addition, miR-340-5p directly bound

to the 3' UTR regions of Bcl-w and Sox2, respectively, as observed via the luciferase assay using wild-type and mutant reporter constructs. The luciferase activities of wild-type Bcl-w/Sox2 reporter and miR-340-5p were significantly decreased relative to those of negative control (NC) miRNA, whereas the luciferase activities of mutant Bcl-w/Sox2 and miR-340-5p constructs were similar to those of the control (Figures 4E and 4F). Since PDGF-A appears to be positively regulated by Bcl-w (Figures 2A–2D), we further investigated the relationship between PDGF-A and miR-340-5p in GBM cells. Overexpression of miR-340-5p led to suppression of PDGF-A as well as Bcl-w and Sox2 expression in GBM cells (Figure 4G).

#### miR-340-5p Suppresses Tumorigenicity in GBM by Directly Repressing Bcl-w and Sox2

The miR-340-5p mimic induced a marked decrease in the levels of EMT-related proteins, including  $\beta$ -catenin, Vimentin, and Twist (Figure 5A), as well as cell migration (Figure 5B) and invasion (Figure 5C) through suppressing the activities of MMP-2 and MMP-9 transcripts (Figure 5D) in U87 and U251 cells, compared with negative control miRNA. miR-340-5p mimic significantly reduced stemness maintenance, including sphere-formation ability and the expression of the cancer stem-like cell markers and angiogenesis-related factor (Figures 5E–5G). Our results suggest that miR-340-5p

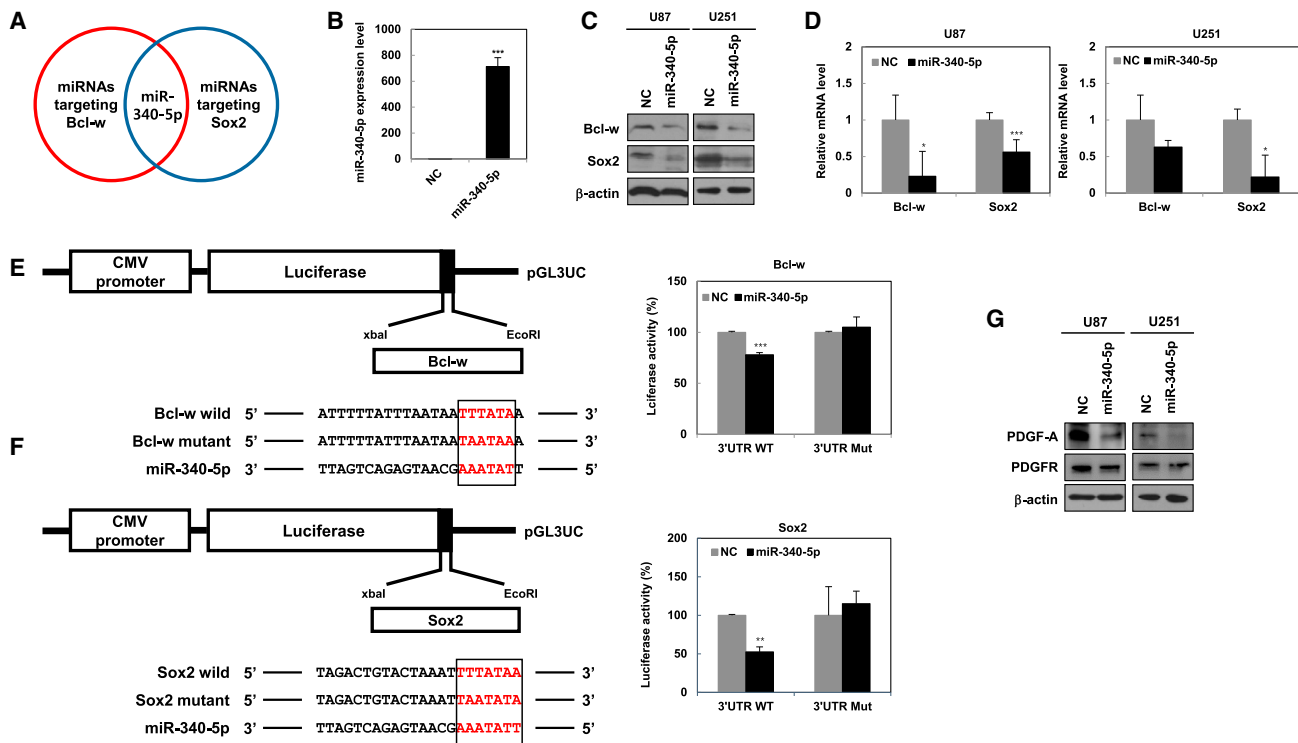


**Figure 4. miR-340-5p Directly Targets Bcl-w and Sox2**

(A) Venn diagram of miRNA targeting Bcl-w and Sox2 was presented through two miRNA prediction sites including TargetScan (<http://www.targetscan.org>) and miRDB (<http://www.mirdb.org>). (B–D) U87 and U251 cells were transfected with negative control or miR-340-5p mimic. (B) miRNA expression level after transfection of miR-340-5p mimic in U251 cells. The levels of Bcl-w and Sox2 protein (C) and mRNA (D) were measured by western blot assay and qRT-PCR analysis, respectively. (E and F) Structure of reporter constructs containing Bcl-w or Sox2 3' UTR downstream of the luciferase ORF. pGL3UC-Bcl-w (E, left) or Sox2 (F, left) vectors containing the wild-type miR-340-5p binding site or a non-binding mutant were constructed. Luciferase activities for reporters with wild or mutant 3' UTR of Bcl-w or Sox2 that co-transfected with the indicated oligonucleotides were measured by dual luciferase assay in the U251 cells. (G) After overexpression of miR-340-5p, PDGF-A protein expression was determined in U87 and U251 cells by western blot assay. The data are presented as the mean ± SD. \*p < 0.05, \*\*p < 0.01, and \*\*\*p < 0.001. Student's t test.

directly downregulates Bcl-w and Sox2 expression to suppress the tumorigenic mechanism in GBM. Additionally, to confirm Bcl-w or Sox2 as targets of miR-340-5p, we showed that the overexpression of Bcl-w or Sox2 rescued the expression of miR-340-5p-decreased malignant-related factors, including Vimentin, Snail, Notch2, and Oct4 in U87 cells (Figure S4). miR-340-5p inhibitor was additionally employed to establish the relationship between miR-340-5p and its target genes, Bcl-w and Sox2. Treatment with the miR-340-5p inhibitor promoted the expression of mesenchymal-related proteins (Figure 6A), migration (Figure 6B), invasion (Figure 6C), sphere-formation ability (Figure 6D), and cancer stem-like markers (Figure 6E), whereas these phenotypes were suppressed by si-Bcl-w and si-Sox2, respectively. Based on the collective data, we propose that miR-340-5p reduces the aggressiveness of GBM by simultaneously suppressing Bcl-w and Sox2 expression.

#### miR-340-5p Negatively Regulates Bcl-w/Sox2 in Patient-Derived Glioma Stem-like Cells and Xenograft Mice

To further confirm whether miR-340-5p attenuates Bcl-w/Sox2-mediated signaling and phenotypes enhancing tumorigenicity, we examined these molecules in patient-derived GSCs (glioma stem-

like cells), including C2M and X08. Bcl-w-overexpressed C2M and X08 cells increased invasiveness, stemness maintenance, and their related factors such as β-catenin, Vimentin, Sox2, and Oct4 expressions (Figures 7A–7C), whereas miR-340-5p significantly repressed these malignant phenotypes (Figures 7D–7F). We also confirmed that miR-340-5p inhibitor increased invasiveness and sphere-formation ability compared to negative control in C2M and X08 cells (Figures S5A and S5B). In patient-derived xenograft mice, X08 cells ( $1 \times 10^4$  cells/mouse, n = 20) were injected into brain of nude mice and kept forming brain tumors for 45 days. Immunohistochemical staining revealed increased Bcl-w and Sox2 expressions in the tumor region (T) compared to adjacent regions (N) of brain tissues (Figure 7G). To validate these results *in vivo*, we analyzed Bcl-w and Sox2 levels in low-grade gliomas and GBM patients. These data were obtained from The Cancer Genome Atlas (TCGA) using cBioPortal for cancer genomics analysis (<http://www.cbioportal.org/>).<sup>29,30</sup> Both Bcl-w and Sox2 showed higher expression levels in GBM than low-grade glioma patients (Figure 7H). Our collective findings suggest that Bcl-w is highly expressed in GBM and promotes secretion of PDGF-A as well as Sox2 activation, leading to aggressive tumorigenesis. miR-340-5p inhibits the aggressiveness

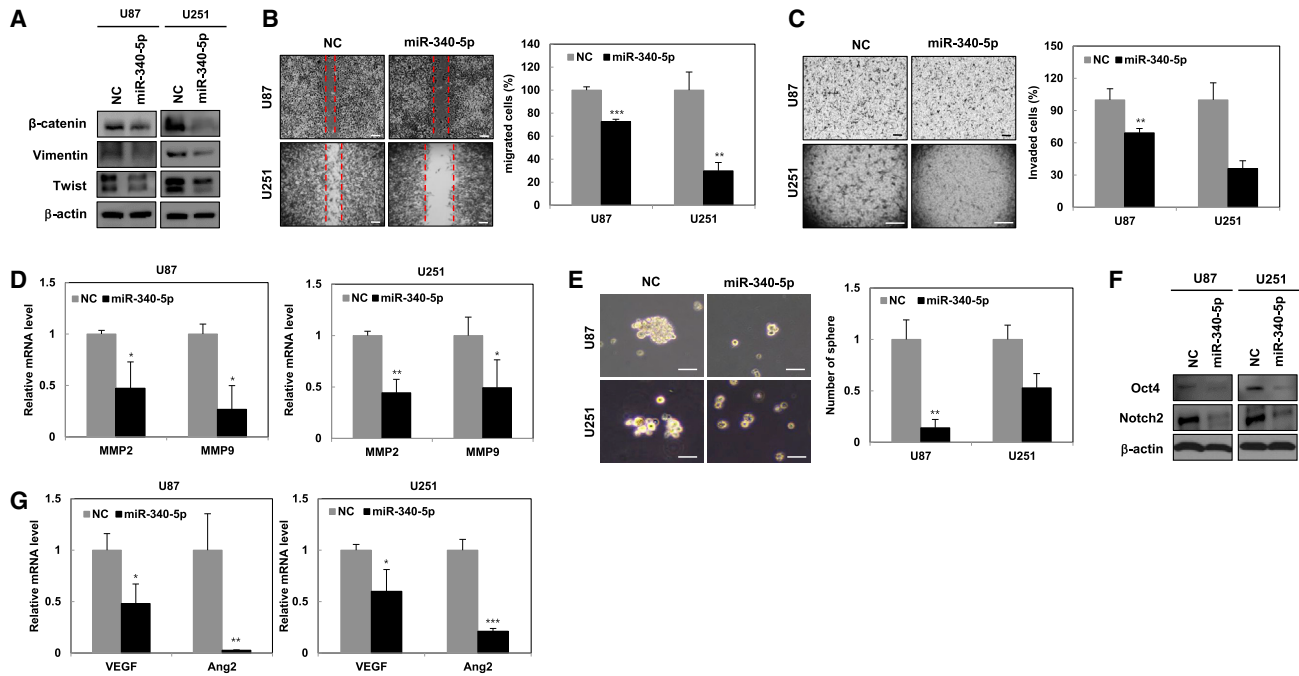


**Figure 5. miR-340-5p Mimic Suppresses Tumorigenicity in U87 and U251 Cells**

(A–G) Mesenchymal-related protein expressions (A), migratory (B) and invasive (C) abilities, MMP-2 and MMP-9 mRNA (D), sphere-formation ability (scale bars, 100  $\mu$ m) (E), cancer stem-like cell-related marker proteins (F), and angiogenesis-related proteins (G) were detected by western blot assay, wound-healing assay (B; scale bars, 100  $\mu$ m), matrigel invasion assay (C; scale bars, 100  $\mu$ m), qRT-PCR, and sphere-formation assay (E; scale bars, 100  $\mu$ m) following transfection of negative control or miR-340-5p mimic in U87 and U251 cells. The data are presented as the mean  $\pm$  SD. \* $p$  < 0.05, \*\* $p$  < 0.01, and \*\*\* $p$  < 0.001. Student's  $t$  test.

of GBM via downregulating Bcl-w, Sox2, and PDGF-A expression (Figure 7I).

In conclusion, Bcl-w-overexpressing GBM cells secrete enhanced levels of PDGF-A owing to changes in the tumor microenvironment, which enhance tumorigenicity. Our novel finding that miR-340-5p functions as a tumor suppressor through attenuation of Bcl-w, Sox2, and PDGF-A highly expressed in GBM supports its utility as a potentially effective therapeutic target for GBM.

## DISCUSSION

Previous studies have demonstrated that Bcl-w contributes to tumorigenicity and metastasis.<sup>11,12</sup> To clarify the mechanism of the aggressive phenotype induced by Bcl-w, we investigated the relationship between Bcl-w-induced PDGF-A and malignancy of GBM in the current study. Our results indicated that changes in the tumor microenvironment triggered by the positive feedback loop of Bcl-w and PDGF-A promote the aggressive characteristics of GBM. Notably, miR-340-5p suppresses the tumorigenic phenotypes of GBM by directly targeting Bcl-w and Sox2 expression and may therefore serve as a potential therapeutic target. The tumor microenvironment consists of tumor cells, immune cells, endothelial cells, and extracellular matrix that produce variable cytokines, chemokines, and growth factors responsible for regulating cell-cell interactions, proliferation, angiogenesis, and metastasis.<sup>31,32</sup> The complex network of secretomes and their receptors con-

tributes to tumor progression or regulation of immune response.<sup>32</sup> In particular, cytokines secreted by tumor cells act as multifunctional proteins involved in cellular activation, angiogenesis, and cell-cell communications, and affect the surrounding microenvironment.<sup>33</sup> Data from this study showed that changes in the tumor microenvironment induced by cytokines secreted from tumor cells lead to aggressive phenotypes related to tumorigenicity and metastasis. Since PDGF-A was determined as one of the major cytokines secreted by Bcl-w, we focused on the correlation between Bcl-w and PDGF-A. PDGF has been identified as a secretome in various cancer cells, including GBM, and may participate in the development of GBM through inducing changes in the tumor microenvironment.<sup>25,34</sup>

We showed which PDGF also contributed to increase Bcl-w expression, leading to aggressive phenotypes of GBM through PDGF receptor (PDGFR) using recombinant PDGF and siRNA against PDGFR (Figure 2). These data were supported by previous studies in which PDGF signaling contributes to implicate the development and progression of GBM and PDGF-derived glioma caused the change of the tumor microenvironment.<sup>34</sup> PDGF led to mesenchymal phenotypes through PDGF receptor (PDGFR).<sup>27</sup> PDGFR is composed of two extracellular domains, and events of intracellular parts were activated by the interaction between the receptors. A number of studies have demonstrated that platelet-derived growth factor receptor alpha (PDGFRA) is highly expressed in all glioma grades, with highest

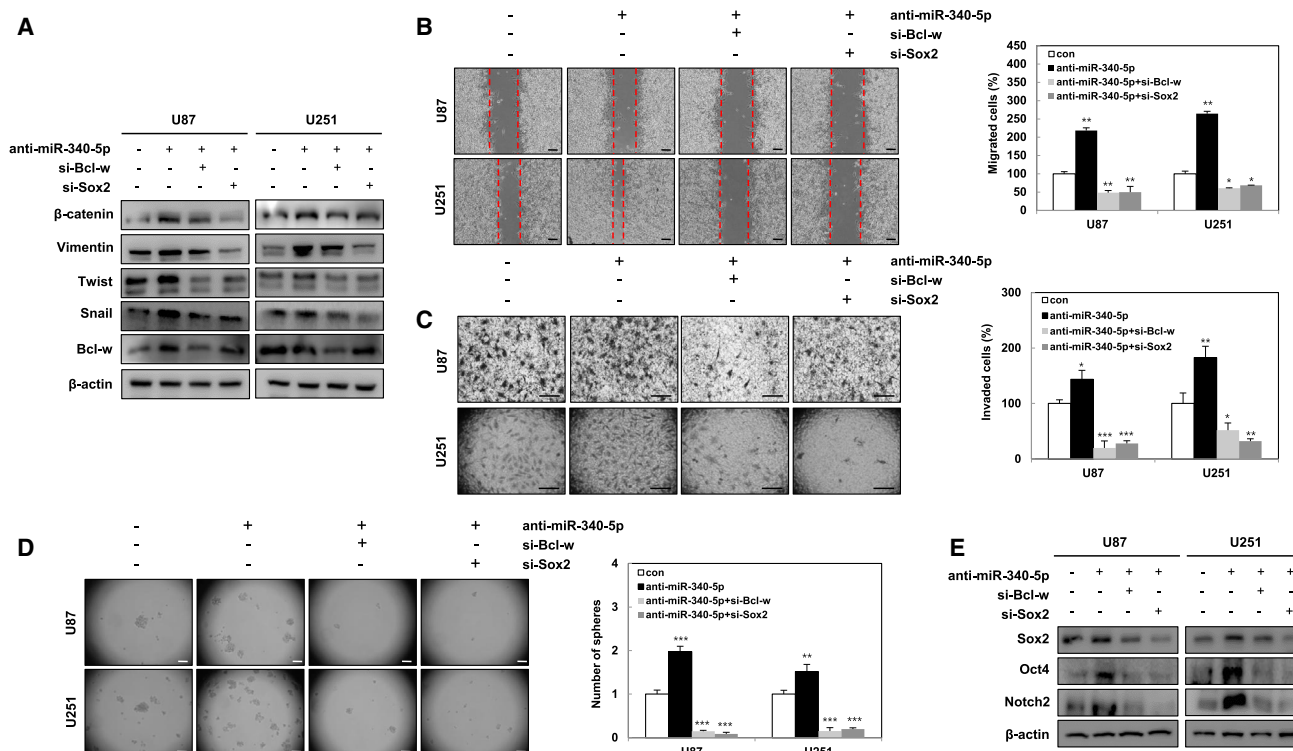


**Figure 6. miR-340-5p Negatively Regulates Aggressiveness via Downregulating Bcl-w and Sox2 Expressions**

(A–E) After being transfected with the indicated miR-340-5p inhibitor (anti-miR-340-5p) or siRNAs against Bcl-w and Sox2, mesenchymal-related protein expressions (A), migratory (B) and invasive (C) abilities, sphere-formation ability (D), and cancer stem-like marker expressions (E) were measured by western blot analysis, wound-healing assay (B; scale bars, 100 μm), matrigel invasion assay (C; scale bars, 100 μm), and sphere-formation assay (D; scale bars, 100 μm) in U87 and U251 cells. The data are presented as the mean ± SD. \**p* < 0.05, \*\**p* < 0.01, and \*\*\**p* < 0.001. Student's *t* test.

detectable levels in glioblastoma.<sup>35,36</sup> The signaling pathways activated through PDGFR induce cell proliferation, survival, and migration, which contribute to individual cellular responses.<sup>27,37</sup>

Several studies have demonstrated high expression of Sox2 and Bcl-w in various cancer types, including GBM.<sup>9,12,38</sup> Interestingly, Sox2, an oncogene, is involved in malignant progression, including invasion and metastasis of cancer cells.<sup>38</sup> Moreover, Bcl-w enhanced tumorigenicity by increasing Sox2 expression (Figure 3). Our major finding was that Bcl-w overexpressed in GBM facilitates the secretion of various cytokines and changes in the tumor microenvironment, ultimately promoting GBM malignancy.

Since miRNAs play crucial roles as gene regulators involved in modulating cell proliferation, survival, and tumorigenesis,<sup>39,40</sup> we focused on miRNAs that inhibit the malignant pathway triggered by Bcl-w and Sox2 activation. Consequently, miR-340-5p was identified as a suppressor simultaneously targeting Bcl-w and Sox2, which attenuated aggressiveness of GBM. This finding is in keeping with an earlier study by our group showing that miR-340 inhibits ionizing radiation-induced metastasis through suppressing interleukin-4 (IL-4) expression in human cancer cells.<sup>16</sup> In the current study, several studies have demonstrated that miR-340-5p exerts anti-tumor efficacy by

suppressing cancer cell progression and stemness maintenance,<sup>41,42</sup> whereas inhibition of miR-340 promotes cancer progression, migration, and invasion.<sup>41,43</sup> Our study also showed that the mesenchymal trait, migratory ability, invasive potential, and stemness maintenance increased by inhibition of miR-340-5p and decreased through suppression of Bcl-w and Sox2 (Figure 6).

Identification of relevant miRNAs and understanding their specific expression patterns and interactions is critical for uncovering potential biomarkers, which provide more effective strategies for diagnosis and therapy of GBM.<sup>44–46</sup> To this end, several miRNAs, including miR-137, miR-203, and miR-429 have been highlighted as diagnostic biomarkers for predicting various cancers.<sup>2,45,47</sup> Based on our current findings, miR-340-5p may serve as a valuable therapeutic target to suppress aggressive GBM tumor growth.

## MATERIALS AND METHODS

### Cell Culture and Chemical Reagents

U87 and U251 (glioblastoma multiforme; GBM) were purchased from the Korea Cell Line Bank (KCLB) and cultured in minimum essential medium (MEM) (Corning, Corning, NY, USA) at 37°C in a humidified atmosphere containing 5% CO<sub>2</sub>. The medium contained 10% fetal bovine serum and 5% penicillin-streptomycin antibiotics (Corning,

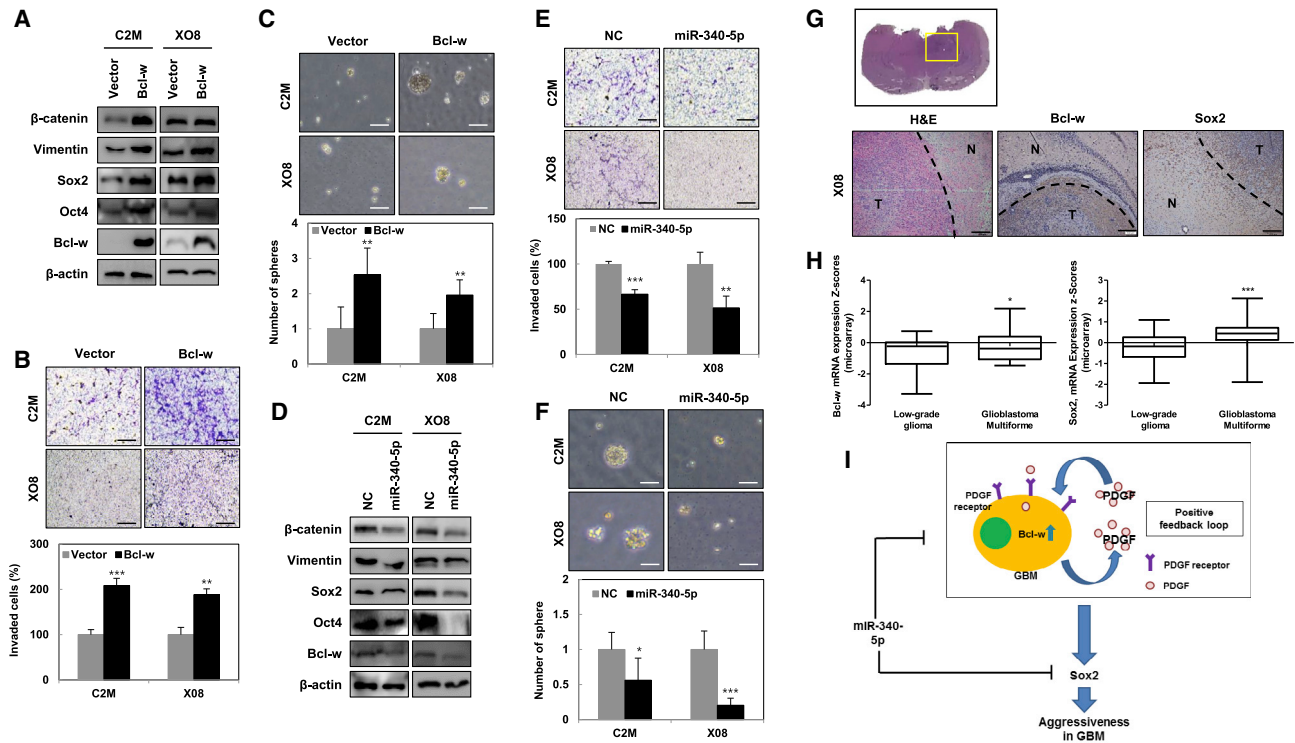


**Figure 7. The Relationship between miR-340-5p and Bcl-w/Sox2 Is Confirmed in Patient-Derived GSCs and Xenograft Mice**

(A–F) Expressions of tumorigenic phenotype-related proteins (A and D), invasive ability (B and E), and stemness maintenance (C and F) were confirmed in Bcl-w or miR-340-5p mimic-overexpressed C2M and X08 cells, patient-derived GSCs by western blot analysis, matrigel invasion assay (scale bars, 100  $\mu$ m), and sphere-formation assay (scale bars, 100  $\mu$ m), respectively. (G) Representative H&E and IHC images for Bcl-w and Sox2 expressions in paraffin-embedded brain tissue of patient-derived xenograft mice using X08 cells (scale bars, 200  $\mu$ m). (H) The expression levels of Bcl-w (TCGA, Provisional) and Sox2 (TCGA, PanCancer Atlas) were compared in low-grade glioma and GBM patients and were obtained from cBioPortal for cancer genomics analysis (<http://www.cbioportal.org>). (I) Schematic diagram in which miR-340-5p suppressed aggressiveness of GBM by inhibiting Bcl-w and Sox2 as well as PDGF-A expression. The data are presented as the mean  $\pm$  SD. \* $p < 0.05$ , \*\* $p < 0.01$ , and \*\*\* $p < 0.001$ . Student's *t* test.

Corning, NY, USA). HUVECs were cultured in endothelial cell growth medium MV2 with supplement mix (Promo Cell, Heidelberg, Germany). Two patient-derived GSCs, C2M and X08, were cultured with DMEM-F-12 (Corning, Corning, NY, USA) containing B27 serum-free supplement (Gibco, Carlsbad, CA, USA), epidermal growth factor (EGF) (Sigma-Aldrich, St. Louis, MO, USA), human fibroblastic growth factor (hFGF) (Biovision, Milpitas, CA, USA), and 5% penicillin-streptomycin antibiotics (Corning). Recombinant human PDGF (R&D Systems, Minneapolis, MN, USA) dissolved in 0.4 mM HCl was treated with Opti MEM medium to cells.

#### Isolation of Patient-Derived GSCs

Patient-derived GSCs, C2M, and X08 cells were generated according to previously published protocol.<sup>48</sup> First, primary tumors removed membrane and blood vessels. After digestion with papain (L-cysteine and EDTA), filtration to a 70- $\mu$ m cell strainer, and centrifugation (300 RCF for 3 min), primary tumor cells were disassociated into single cells. Disassociated single cells were cultured with DMEM/F-12 media supplemented with N2 supplements, EGF, basic fibroblast growth factor (bFGF), and penicillin-streptomycin antibiotics. Isolated GSCs were identified by CD133 expression.

#### RNAs, Plasmid DNAs, and Transfection

miR-340-5p mimic, miR-340-5p inhibitor, and negative control were purchased from Genolution (Seoul, Korea). miR-340-5p (5'-UUAUAAAGCAAUGAGACUGAUU-3') and negative control (5'-UUCUCCG AACGUGACGUTT-3') were constructed as a double strand. siRNA duplex oligonucleotides targeting Sox2 (sc-38408) and Bcl-w (sc-37293) were purchased from Santa Cruz Biotechnology (Dallas, TX, USA). Control was synthesized by Genolution (Seoul, Korea) as double-strand RNA designed from the sequences (5'-UCGU UAAUCGGCUAAUACGC-3'). pcDNA-3.1 vector containing Bcl-w and pCMV-Tag2 vector containing Sox2 was used as transiently transfected for producing overexpressing cells. siRNA, miRNA, and plasmid DNA were transfected to U251 or U87 cells using Lipofectamine 2000 reagent (Invitrogen, Carlsbad, CA, USA) for 48 h.

#### RNA Extraction and Quantitative Real-Time PCR

Total RNA was extracted by Trizol reagent (Favorgen Biotech, Ping-Tung, Taiwan) following the manufacturer's introduction. The cDNAs were synthesized by a mixture with Tetro cDNA synthesis kit (Bioline, London, UK). In addition, the miRNAs were synthesized using Mir-X miRNA qRT-PCR SYBR kit (Clontech Laboratories,



Mountain View, CA, USA). The mRNA and miRNA levels were determined using iCycler real-time PCR detection system (Roche, Basel, Switzerland) following to the manufacturer's instructions. The primers of glyceraldehyde 3-phosphate dehydrogenase (GAPDH) and U6 were used for normalized mRNA and miRNA, respectively. The sequences of the primers were as follows: MMP-2, 5'-CATCAAGGGCATTTCAGGAGC-3' (forward) and 5'-AGAACA CAGCCTTCTCCTCC-3' (reverse); MMP-9, 5'-AGGACGACGTG AATGGC ATG-3' (forward) and 5'-ATCGTCCACCGGACTCA AAG-3' (reverse); VEGF, 5'-GAC AGACAGACAGACACCGCC-3' (forward) and 5'-GAACAGCCCAGAAGTTGGACG-3' (reverse); Ang2, 5'-ATGGGTCCTGCAGCTACACT-3' (forward) and 5'-CTC TGCACCGA GTCATCGTA-3' (reverse); Sox2, 5'-ATGCACCGCTA CGACGTGA-3' (forward) and 5'-CTTTTGCACCCCTCCCATT-3' (reverse); EGFR, 5'-TCCCCGTAATTATGTGGTGAC AGA-3' (forward) and 5'-ACCCCTAAATGCCACCGGC-3' (reverse); PDGFA, 5'-CAC ACCTCCTCGCTGTAGTATTTA-3' (forward) and 3'-GTT ATCGGTGTAAATGTCATC CAA-3' (reverse); MCP-3, 5'-CTT CTGTGTCTGCTGCTCAC-3' (forward) and 5'-GGG TCAGCAC AGATCTCCTT-3' (reverse); Bcl-w, 5'-GGACAAGTGCAGGAG TGGAT-3' (forward) and 5'-GTCCTCACTGATGCCAGTT-3' (reverse); miR-340-5p, 5'-TTATAA AGCAATGAGACTGATT-3'; and GAPDH, 5'-CATCTCTGCCCCCTCTGCTGA-3' (forward) and 5'-GGATGACCTTGCCCCACAGCCT-3' (reverse).

#### Wound-Healing Assay

The U87 and U251 confluent cell monolayers were scratched across the 6-well plates using a yellow tip. Cells were washed with PBS and incubated for 16 h to allow migration. The cell morphology was captured using a microscope and fixed with methanol. The samples were stained with 0.05% crystal violet in 10% methanol.

#### Matrigel Invasion Assay

The cells were placed in the upper matrigel-coated transwell chambers (8  $\mu$ m pore) (Corning), and the lower chamber containing 10% fetal bovine serum (FBS) media. The invasion assay was performed following the manufacturer's instructions. The stained cells were obtained under a light microscope (Olympus, Tokyo, Japan).

#### Dual Luciferase Reporter Assay

pGL3UC vector constructs kindly was provided by V.N. Kim (School of Biological Sciences, Seoul National University, Korea).<sup>49</sup> A DNA fragment of human Bcl-w 3' UTR containing the putative miR-340-5p binding site (88 bp) was constructed and cloned into pGL3UC. The nucleotide sequences of primers for the amplification of the Bcl-w 3' UTRs were 5'- AAATGCTCTAGAGCCTATA TTCCTGTATTTTTATTTAATAATTTATAAA-3' (forward) and 5'-ACACGGAATTCAAAAAATAAAAGTCAAATGAACTTGGA TTTATAAATT-3' (reverse), and the Sox2 3' UTRs were 5'-AAAA GCTCTAGAGCGGGCAAAAGTTTTAGACT GTACTAAATTTT ATAAC-3' (forward) and 5'-CCTGGGAATTCATGGCCATTT TGGCT TTAAACAGTAAGTTATAAAAT-3' (reverse), which contained the binding site of miR-340-5p (TTTATA). The vector of mutant type is constructed out of "AATA" that have site-directed

mutagenesis of the Bcl-w and Sox2 3' UTR for binding of miR-340-5p. Then pGL3UC vector were cut by XbaI and EcoRI restriction enzymes, and fragment of PCR product was ligated into pGL3UC vector.

U251 cells were transfected with reporter plasmid containing Bcl-w or Sox2 (200 ng), pRL-CMV-Renilla (Promega, Madison, WI, USA) plasmid (1 ng), and miR-340-5p using Lipofectamine 2000 (Thermo Fisher Scientific, Waltham, MA, USA) in 24-well plates. Luciferase reporter system (Promega) was performed according to manufacturer's protocol. Renilla luciferase activity was used as normalization.

#### Immunofluorescence Staining

The cells transfected with empty vector or that contained Bcl-w were seeded on slide glasses and incubated for 48 h. The slides were fixed with 4% paraformaldehyde for 10 min at room temperature and incubated with the primary antibodies including Sox2 and Bcl-w (Cell Signaling, Beverly, MA, USA) overnight and then washed with PBS three times. The samples were incubated with the secondary fluorescence-conjugated antibodies (Invitrogen, Carlsbad, CA, USA) and stained with DAPI in PBS. The samples were mounted by ProLong Gold antifade reagent (Invitrogen, Carlsbad, CA, USA) and assessed with a confocal laser scanning microscope (CLSM; Carl Zeiss, Oberkochen, Germany).

#### Patient-Derived Xenograft Model

X08 cells were transplanted following resuspension in DMEM/F-12 with B27, EGF, and hFGF. X08 cells ( $1 \times 10^4$  cells/mouse, n = 20) were orthotopically injected into the left striatum of 5-week-old female BALB/c nude mice. The brain of each mouse was obtained 45 days after injection. Brain samples were fixed in 4% paraformaldehyde for H&E and immunohistochemistry staining. This study was reviewed and approved by the Institutional Animal Care and Use Committee (IACUC) of Korea Institute of Radiological and Medical Science.

#### H&E and Immunohistochemistry (IHC) Staining

The brain tissue was sectioned and deparaffinized and rehydrated with antigen retrieval. The slides were stained using H&E (Thermo Fisher Scientific). In IHC, primary antibodies were immunoblotting using anti-Bcl-w (Abcam, Cambridge, UK) and anti-Sox2 (Santa Cruz Biotechnology) overnight at 4°C. After washing with Tris buffered saline with Tween 20 (TBST), ABC (avidin-biotin complex) and 3,3'-diaminobenzidine (DAB) kit (Vector Laboratory, Burlingame, CA, USA) were performed following manufacturer's protocols. The samples were observed and photographed by a cellSens (Olympus).

#### Tube-Formation Assay

The 96-well plates were coated with matrigel (BD Biosciences, San Jose, CA, USA).  $4 \times 10^4$  HUVECs (human umbilical vein endothelial cells) with 1% FBS media were seeded on the top of matrigel layers and incubated for 6 h. The tube length was analyzed and counted from 3 difference fields using an invert microscope.

### Sphere-Formation Assay

For the sphere-formation assay, cells ( $1 \times 10^3$  /well) were seeded with DMEM-F-12 (Corning) containing B27 serum-free supplement (50×; Gibco) and 5% penicillin-streptomycin for 7–10 days. After 7–10 days, spheres with a diameter  $> 20 \mu\text{m}$  were counted.

### Western Blot Assay

U87, U251, C2M, and X08 cells were collected and lysed with RIPA buffer supplemented with protease and phosphatase inhibitors (Roche, Basel, Switzerland). Protein extraction and western blot were conducted as previously described.<sup>9,16</sup> The primary antibodies used as follows:  $\beta$ -catenin, Bcl-w, Notch2, Oct4, Snail, Vimentin, phospho-ERK, and Sox2 were purchased from Cell Signaling. Twist was purchased from Abcam (Cambridge, UK). ERK, PDGF-A, PDGFR- $\alpha$ , phospho-JNK, JNK, phospho-p38, p38, Slug, Sox2, VEGF, Ang2, and  $\beta$ -actin were purchased from Santa Cruz Biotechnology. The secondary antibodies were anti-rabbit and anti-mouse immunoglobulin G-horseradish peroxidase (IgG-HRP) (Bio-Rad, Hercules, CA, USA).

### Statistical Analysis

All data were analyzed by GraphPad statistical software.  $p < 0.05$  was considered as significant, whereas  $p < 0.01$  and  $< 0.001$  were highly considered statistically significant, respectively.

### SUPPLEMENTAL INFORMATION

Supplemental Information can be found online at <https://doi.org/10.1016/j.omtn.2019.05.022>.

### AUTHOR CONTRIBUTIONS

I.H.B. supervised the work; S.K. and J.Y.C. performed research and analyzed data; I.H.B., S.K., J.Y.C., and H.J.S. designed the experiments and drafted the manuscript. I.H.B., M.-J.P., and H.Y.C. designed and performed animal experiments. All authors discussed the results and commented on the manuscript.

### CONFLICTS OF INTEREST

The authors declare no potential conflicts of interest.

### ACKNOWLEDGMENTS

Patient-derived GSC, X08 cells were kindly provided by Deric M. Park at the National Cancer Institute (Bethesda, MD, USA). This study was supported by a grant from the Korea Institute of Radiological and Medical Sciences (KIRAMS) and funded by the Basic Science Research Program through the National Research Foundation of Korea (NRF) and Ministry of Science and ICT (MSIT), Republic of Korea. (no. NRF-2017M2A2A7A01018542(50035-2019); 50531-2019).

### REFERENCES

- Ahir, B.K., Ozer, H., Engelhard, H.H., and Lakka, S.S. (2017). MicroRNAs in glioblastoma pathogenesis and therapy: A comprehensive review. *Crit. Rev. Oncol. Hematol.* *120*, 22–33.
- Chen, J., Yang, L., and Wang, X. (2017). Reduced circulating microRNA-203 predicts poor prognosis for glioblastoma. *Cancer Biomark.* *20*, 521–526.
- Banelli, B., Forlani, A., Allemanni, G., Morabito, A., Pistillo, M.P., and Romani, M. (2017). MicroRNA in glioblastoma: An overview. *Int. J. Genomics* *2017*, 7639084.
- Liu, X., Gao, Q., Zhao, N., Zhang, X., Cui, W., Sun, J., Fu, J., and Hao, J. (2018). Sohlh1 suppresses glioblastoma cell proliferation, migration, and invasion by inhibition of Wnt/ $\beta$ -catenin signaling. *Mol. Carcinog.* *57*, 494–502.
- Chung, H.J., Choi, Y.E., Kim, E.S., Han, Y.H., Park, M.J., and Bae, I.H. (2015). miR-29b attenuates tumorigenicity and stemness maintenance in human glioblastoma multiforme by directly targeting BCL2L2. *Oncotarget* *6*, 18429–18444.
- Hoelzinger, D.B., Mariani, L., Weis, J., Woyke, T., Berens, T.J., McDonough, W.S., Sloan, A., Coons, S.W., and Berens, M.E. (2005). Gene expression profile of glioblastoma multiforme invasive phenotype points to new therapeutic targets. *Neoplasia* *7*, 7–16.
- Chen, W., Xia, T., Wang, D., Huang, B., Zhao, P., Wang, J., Qu, X., and Li, X. (2016). Human astrocytes secrete IL-6 to promote glioma migration and invasion through upregulation of cytomembrane MMP14. *Oncotarget* *7*, 62425–62438.
- Li, G., Qin, Z., Chen, Z., Xie, L., Wang, R., and Zhao, H. (2017). Tumor Microenvironment in Treatment of Glioma. *Open Med. (Wars.)* *12*, 247–251.
- Bae, I.H., Park, M.-J., Yoon, S.H., Kang, S.W., Lee, S.-S., Choi, K.-M., and Um, H.D. (2006). Bcl-w promotes gastric cancer cell invasion by inducing matrix metalloproteinase-2 expression via phosphoinositide 3-kinase, Akt, and Sp1. *Cancer Res.* *66*, 4991–4995.
- Wilson, J.W., Nostro, M.C., Balzi, M., Faraoni, P., Cianchi, F., Becciolini, A., and Potten, C.S. (2000). Bcl-w expression in colorectal adenocarcinoma. *Br. J. Cancer* *82*, 178–185.
- Lee, W.S., Kwon, J., Yun, D.H., Lee, Y.N., Woo, E.Y., Park, M.J., Lee, J.S., Han, Y.H., and Bae, I.H. (2014). Specificity protein 1 expression contributes to Bcl-w-induced aggressiveness in glioblastoma multiforme. *Mol. Cells* *37*, 17–23.
- Lee, W.S., Woo, E.Y., Kwon, J., Park, M.J., Lee, J.S., Han, Y.H., and Bae, I.H. (2013). Bcl-w Enhances Mesenchymal Changes and Invasiveness of Glioblastoma Cells by Inducing Nuclear Accumulation of  $\beta$ -Catenin. *PLoS ONE* *8*, e68030.
- Lin, C.-W., Chang, Y.-L., Chang, Y.-C., Lin, J.-C., Chen, C.-C., Pan, S.-H., Wu, C.T., Chen, H.Y., Yang, S.C., Hong, T.M., and Yang, P.C. (2013). MicroRNA-135b promotes lung cancer metastasis by regulating multiple targets in the Hippo pathway and LZTS1. *Nat. Commun.* *4*, 1877.
- Shi, Z.M., Wang, L., Shen, H., Jiang, C.F., Ge, X., Li, D.M., Wen, Y.Y., Sun, H.R., Pan, M.H., Li, W., et al. (2017). Downregulation of miR-218 contributes to epithelial-mesenchymal transition and tumor metastasis in lung cancer by targeting Slug/ZEB2 signaling. *Oncogene* *36*, 2577–2588.
- Shenouda, S.K., and Alahari, S.K. (2009). MicroRNA function in cancer: oncogene or a tumor suppressor? *Cancer Metastasis Rev.* *28*, 369–378.
- Kim, E.S., Choi, Y.E., Hwang, S.J., Han, Y.-H., Park, M.-J., and Bae, I.H. (2016). IL-4, a direct target of miR-340/429, is involved in radiation-induced aggressive tumor behavior in human carcinoma cells. *Oncotarget* *7*, 86836–86856.
- Yuan, X., Curtin, J., Xiong, Y., Liu, G., Waschmann-Hogiu, S., Farkas, D.L., Black, K.L., and Yu, J.S. (2004). Isolation of cancer stem cells from adult glioblastoma multiforme. *Oncogene* *23*, 9392–9400.
- Pastrana, E., Silva-Vargas, V., and Doetsch, F. (2011). Eyes wide open: a critical review of sphere-formation as an assay for stem cells. *Cell Stem Cell* *8*, 486–498.
- Yata, K., Beder, L.B., Tamagawa, S., Hotomi, M., Hirohashi, Y., Grenman, R., and Yamanaka, N. (2015). MicroRNA expression profiles of cancer stem cells in head and neck squamous cell carcinoma. *Int. J. Oncol.* *47*, 1249–1256.
- Ma, J., Xia, J., Miele, L., Sarkar, F.H., and Wang, Z. (2013). Notch signaling pathway in pancreatic cancer progression. *Pancreat. Disord. Ther.* *3*, 1000114.
- Bradshaw, A., Wickremesekera, A., Brasch, H.D., Chibnall, A.M., Davis, P.F., Tan, S.T., and Itinteang, T. (2016). Cancer stem cells in glioblastoma multiforme. *Front. Surg.* *3*, 48.
- Neradil, J., and Veselska, R. (2015). Nestin as a marker of cancer stem cells. *Cancer Sci.* *106*, 803–811.
- Brescia, P., Ortensi, B., Fornasari, L., Levi, D., Broggi, G., and Pelicci, G. (2013). CD133 is essential for glioblastoma stem cell maintenance. *Stem Cells* *31*, 857–869.

24. Murata, T., Mizushima, H., Chinen, I., Moribe, H., Yagi, S., Hoffman, R.M., Kimura, T., Yoshino, K., Ueda, Y., Enomoto, T., and Mekada, E. (2011). HB-EGF and PDGF mediate reciprocal interactions of carcinoma cells with cancer-associated fibroblasts to support progression of uterine cervical cancers. *Cancer Res.* *71*, 6633–6642.
25. Hwang, D.L., Latus, L.J., and Lev-Ran, A. (1992). Effects of platelet-contained growth factors (PDGF, EGF, IGF-I, and TGF- $\beta$ ) on DNA synthesis in porcine aortic smooth muscle cells in culture. *Exp. Cell Res.* *200*, 358–360.
26. Shikada, Y., Yonemitsu, Y., Koga, T., Onimaru, M., Nakano, T., Okano, S., Sata, S., Nakagawa, K., Yoshino, L., Maehara, Y., and Sueishi, K. (2005). Platelet-derived growth factor-AA is an essential and autocrine regulator of vascular endothelial growth factor expression in non-small cell lung carcinomas. *Cancer Res.* *65*, 7241–7248.
27. Heldin, C.-H. (2013). Targeting the PDGF signaling pathway in tumor treatment. *Cell Commun. Signal.* *11*, 97.
28. Shao, M., Rossi, S., Chelladurai, B., Shimizu, M., Ntukogu, O., Ivan, M., Calin, G.A., and Matei, D. (2011). PDGF induced microRNA alterations in cancer cells. *Nucleic Acids Res.* *39*, 4035–4047.
29. Gao, J., Aksoy, B.A., Dogrusoz, U., Dresdner, G., Gross, B., Sumer, S.O., Sun, Y., Jacobsen, A., Sinha, R., Larsson, E., et al. (2013). Integrative analysis of complex cancer genomics and clinical profiles using the cBioPortal. *Sci. Signal.* *6*, p11.
30. Cerami, E., Gao, J., Dogrusoz, U., Gross, B.E., Sumer, S.O., Aksoy, B.A., Jacobsen, A., Byrne, C.J., Heuer, M.L., Larsson, E., et al. (2012). The cBio cancer genomics portal: an open platform for exploring multidimensional cancer genomics data. *Cancer Discov.* *2*, 401–404.
31. Albulescu, R., Codrici, E., Popescu, I.D., Mihai, S., Necula, L.G., Petrescu, D., Teodoru, M., and Tanase, C.P. (2013). Cytokine patterns in brain tumour progression. *Mediators Inflamm.* *2013*, 979748.
32. Iwami, K., Natsume, A., and Wakabayashi, T. (2011). Cytokine networks in glioma. *Neurosurg. Rev.* *34*, 253–263, discussion 263–264.
33. Zisakis, A., Piperi, C., Themistocleous, M.S., Korkolopoulou, P., Boviatsis, E.I., Sakas, D.E., Patsouris, E., Lea, R.W., and Kalofoutis, A. (2007). Comparative analysis of peripheral and localised cytokine secretion in glioblastoma patients. *Cytokine* *39*, 99–105.
34. Nazarenko, I., Hede, S.-M., He, X., Hedrén, A., Thompson, J., Lindström, M.S., and Nistér, M. (2012). PDGF and PDGF receptors in glioma. *Ups. J. Med. Sci.* *117*, 99–112.
35. Fredriksson, L., Li, H., and Eriksson, U. (2004). The PDGF family: four gene products form five dimeric isoforms. *Cytokine Growth Factor Rev.* *15*, 197–204.
36. Kim, Y., Kim, E., Wu, Q., Guryanova, O., Hitomi, M., Lathia, J.D., Serwanski, D., Sloan, A.E., Weil, R.J., Lee, J., et al. (2012). Platelet-derived growth factor receptors differentially inform intertumoral and intratumoral heterogeneity. *Genes Dev.* *26*, 1247–1262.
37. Andrae, J., Gallini, R., and Betsholtz, C. (2008). Role of platelet-derived growth factors in physiology and medicine. *Genes Dev.* *22*, 1276–1312.
38. Avilion, A.A., Nicolis, S.K., Pevny, L.H., Perez, L., Vivian, N., and Lovell-Badge, R. (2003). Multipotent cell lineages in early mouse development depend on SOX2 function. *Genes Dev.* *17*, 126–140.
39. Gabrieli, G., Yi, M., Narayan, R.S., Niers, J.M., Wurdinger, T., Imitola, J., Ligon, K.L., Kesari, S., Esau, C., Stephens, R.M., et al. (2011). Human glioma growth is controlled by microRNA-10b. *Cancer Res.* *71*, 3563–3572.
40. Gao, Y.T., Chen, X.B., and Liu, H.L. (2016). Up-regulation of miR-370-3p restores glioblastoma multiforme sensitivity to temozolomide by influencing MGMT expression. *Sci. Rep.* *6*, 32972.
41. Shi, Z., Li, Y., Qian, X., Hu, Y., Liu, J., Zhang, S., and Zhang, J. (2017). MiR-340 Inhibits Triple-Negative Breast Cancer Progression by Reversing EZH2 Mediated miRNAs Dysregulated Expressions. *J. Cancer* *8*, 3037–3048.
42. Raychaudhuri, M., Bronger, H., Buchner, T., Kiechle, M., Weichert, W., and Avril, S. (2017). MicroRNAs miR-7 and miR-340 predict response to neoadjuvant chemotherapy in breast cancer. *Breast Cancer Res. Treat.* *162*, 511–521.
43. Wang, N., Xiang, X., Chen, K., Liu, P., and Zhu, A. (2018). Targeting of NT5E by miR-30b and miR-340 attenuates proliferation, invasion and migration of gallbladder carcinoma. *Biochimie* *146*, 56–67.
44. McGuire, A., Brown, J.A., and Kerin, M.J. (2015). Metastatic breast cancer: the potential of miRNA for diagnosis and treatment monitoring. *Cancer Metastasis Rev.* *34*, 145–155.
45. Dong, H., Hao, X., Cui, B., and Guo, M. (2017). MiR-429 suppresses glioblastoma multiforme by targeting SOX2. *Cell Biochem. Funct.* *35*, 260–268.
46. Liao, H., Bai, Y., Qiu, S., Zheng, L., Huang, L., Liu, T., Wang, X., Liu, Y., Xu, N., Yan, X., and Guo, H. (2015). MiR-203 downregulation is responsible for chemoresistance in human glioblastoma by promoting epithelial-mesenchymal transition via SNAI2. *Oncotarget* *6*, 8914–8928.
47. Li, H.Y., Li, Y.M., Li, Y., Shi, X.W., and Chen, H. (2016). Circulating microRNA-137 is a potential biomarker for human glioblastoma. *Eur. Rev. Med. Pharmacol. Sci.* *20*, 3599–3604.
48. Jung, J., Gilbert, M.R., and Park, D.M. (2016). Isolation and propagation of glioma stem cells from acutely resected tumors. *Methods Mol. Biol.* *1516*, 361–369.
49. Park, S.-Y., Lee, J.H., Ha, M., Nam, J.-W., and Kim, V.N. (2009). miR-29 miRNAs activate p53 by targeting p85  $\alpha$  and CDC42. *Nat. Struct. Mol. Biol.* *16*, 23–29.